Materials Science and Engineering B 137 (2007) 289–294

www.elsevier.com/locate/mseb

Short communication

Chalcogen doping of silicon via intense femtosecond-laser irradiation

Michael A. Sheehy [a,1], Brian R. Tull [b,*], Cynthia M. Friend [a,b,1,2], Eric Mazur [b,2]

[a] *Department of Chemistry & Chemical Biology, Harvard University, 12 Oxford Street, Mb22, Cambridge, MA 02138, United States*
[b] *Division of Engineering and Applied Sciences, Harvard University, 9 Oxford Street, Cambridge, MA 02138, United States*

Received 1 June 2006; received in revised form 2 October 2006; accepted 8 October 2006

Abstract

We have previously shown that doping silicon with sulfur via femtosecond-laser irradiation leads to near-unity absorption of radiation from ultraviolet wavelengths to below band gap short-wave infrared wavelengths. Here, we demonstrate that doping silicon with two other group VI elements (chalcogens), selenium and tellurium, also leads to near-unity broadband absorption. A powder of the chalcogen dopant is spread on the silicon substrate and irradiated with femtosecond-laser pulses. We examine and compare the resulting morphology, optical properties, and chemical composition for each chalcogen-doped substrate before and after thermal annealing. Thermal annealing reduces the absorption of below band gap radiation by an amount that correlates with the diffusivity of the chalcogen dopant used to make the sample. We propose a mechanism for the absorption of below band gap radiation based on defects in the lattice brought about by the femtosecond-laser irradiation and the presence of a supersaturated concentration of chalcogen dopant atoms. The selenium and tellurium doped samples show particular promise for use in infrared photodetectors as they retain most of their infrared absorptance even after thermal annealing—a necessary step in many semiconductor device manufacturing processes.

Keywords: Silicon; Infrared absorption; Doping and impurity implantation; Femtosecond pulsed laser ablation

1. Introduction

Recently we reported on the unique optoelectronic properties of highly sulfur-doped laser-microstructured silicon [1,2]. Doping silicon with sulfur, and other group VI elements (chalcogens), is studied for its potential impact on improving silicon-based infrared photodetectors [2–4], light emitting diodes [5–9] and thin-film photovoltaics [10–13]. Research on the nature of the chalcogen dopant in the silicon lattice and resulting material properties has been performed using ion implantation [4,6,14–17] and vapor diffusion [6,8,18–20] followed by furnace annealing. Doping by either of these methods restricts the chalcogen concentration in the lattice to the solid solubility limit. However, a supersaturated solution can be created when the annealing of ion-implanted material is performed with short laser pulses [17] or when material is irradiated with short laser pulses in a gaseous environment [21]. Here we create high concentrations of chalcogen dopants in silicon samples using irradiation with femtosecond-laser pulses resulting in near-unity absorptance of below band gap radiation. The resulting chalcogen dopants contained within the lattice at supersaturated concentrations cause significant absorptance of below band gap radiation.

We have previously shown that irradiation of single crystal silicon with femtosecond-laser pulses at a fluence above the ablation threshold (as in the experiment presented here) results in the formation of a microstructured surface layer with interesting optical properties [22–27]. This surface layer is several hundred nanometers thick and is composed of polycrystalline silicon with a grain size ranging from 10 to 50 nm [23]. When irradiation is performed in a background gas, the microstructured surface layer is doped with a high concentration of atoms from the background gas (about 1%) [1]. The morphology and optical properties vary greatly with background gas chemistry. When the background gas contains sulfur, the microstructured silicon exhibits near-unity absorption of radiation from 250 to 2500 nm which includes the below band gap near infrared; in contrast, crystalline silicon is nearly transparent to wavelengths longer than 1100 nm [24].

* Corresponding author. Fax: +1 617 496 4654.
E-mail address: tull@fas.harvard.edu (B.R. Tull).
[1] Fax: +1 617 496 8410.
[2] Fax: +1 617 496 4654.

0921-5107/$ – see front matter © 2006 Published by Elsevier B.V.
doi:10.1016/j.mseb.2006.10.002

In this work, we introduce the dopant into the microstructuring process as a powder spread on the surface of a silicon wafer, rather than as a background gas. Using a powder allows us to explore other dopants that are not convenient to work with in gaseous form. Using this method, we identify two other chalcogens in addition to sulfur, which also yield absorption of below band gap near infrared light: selenium and tellurium. We examine the resulting morphology, dopant concentration and optical properties of the substrates microstructured in the presence of each element before and after thermal annealing. Based on the results, we comment on the role of the chalcogen dopant on the absorption of below band gap near infrared radiation.

2. Experimental

For all experiments, we used a high resistivity ($\rho = 8$–$12\,\Omega\,\mathrm{m}$), *n*-doped Si(1 1 1) substrate wafer cut to a size of 10 mm × 10 mm. Approximately 2 mg of the desired dopant, in powder form, was placed on the silicon wafer and manually dispersed across the surface using 0.5 mL of either toluene (for sulfur and selenium) or mineral oil (for tellurium). The solvent evaporates and the powder remains adhered to the silicon surface. We then placed the sample in a stainless steel chamber and evacuated the chamber to less than 6.7 Pa using a corrosion-resistant mechanical pump. The chamber was then filled with 6.7×10^4 Pa of N_2.

We irradiated the samples with a 1-kHz train of 100-fs, 800-nm laser pulses with a fluence of $10\,\mathrm{kJ\,m^{-2}}$ focused to a spot size of 150 μm in diameter. The sample is raster-scanned at $250\,\mu\mathrm{m\,s^{-1}}$ and stepped vertically 50 μm at the end of each row so that all areas of the silicon receive uniform exposure to the laser. After irradiation, samples are placed in an ultrasonic bath of methanol for 30 min to remove any powder residue. We thermally annealed samples in a vacuum oven at 775 K for 30 min to analyze changes in morphology, composition, and absorptance that occur with heating. The base pressure of the annealing oven never exceeded 4.0×10^{-4} Pa.

To evaluate the optical properties of the samples, we measured the infrared absorptance with a UV–vis–NIR spectrophotometer equipped with an integrating sphere detector. The reflectance (R) and transmittance (T) were measured for wavelengths in the range of 0.25–2.5 μm, in 1-nm increments to determine the absorptance ($A = 1 - R - T$) at each wavelength.

To measure the composition of the substrates after irradiation, we used Rutherford backscattering spectrometry (RBS). Before each measurement, we dipped the samples for 10 min in a 10% HF solution to remove any oxide layer. The backscattering measurements were taken with 2.0-MeV alpha particles and an annular solid-state detector. We fitted our data to simulated spectra to determine the composition of the samples.

3. Results

Fig. 1 shows scanning electron microscope images of surfaces irradiated in the presence of sulfur, selenium and tellurium powder. For comparison, Fig. 1d shows the surface after irradiation in sulfur hexafluoride gas (taken from Ref. [1]). The conical structures formed in the presence of a powder are roughly twice as large and half as dense as those formed in sulfur hexafluoride gas. The height of the structures is between 9 and 14 μm; the width on the long axis varies from 6 to 9 μm; and the width on the short axis ranges from 2 to 3 μm. The sulfur and tellurium microstruc-

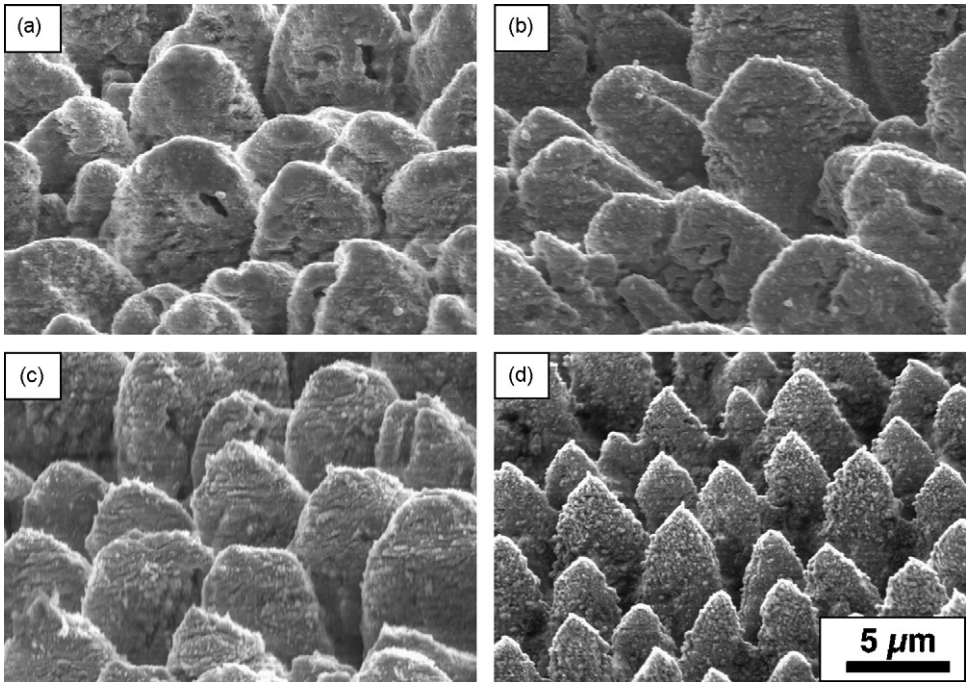

Fig. 1. Scanning electron microscope images of irradiated surfaces using (a) sulfur powder, (b) selenium powder, (c) tellurium powder and (d) sulfur hexafluoride gas as a dopant source. In each image the surface is at a 45° angle and the long axis of the structures' elliptical base is parallel to the plane of the image. Subpart (d) is taken from Ref. [1].

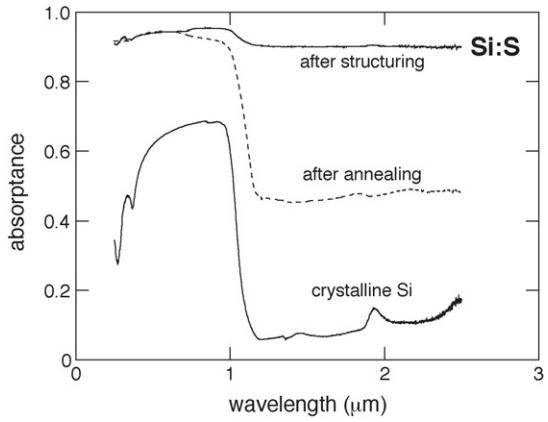

Fig. 2. Absorptance spectra for a sample doped with sulfur before annealing (solid line), and after annealing to 775 K for 30 min (dashed line). The absorptance of an untreated silicon wafer is included for comparison.

tures have some nanoscale texture; the selenium microstructures are smooth in comparison. There is no change in morphology after annealing to the resolution of the scanning electron microscope.

Figs. 2–4 compares the absorptance for samples created in sulfur, selenium and tellurium to that of crystalline silicon before and after the samples are annealed. All samples have 90% absorptance at wavelengths from 1.2 to 2.5 μm before annealing; the absorptance for a non-irradiated crystalline silicon wafer at these wavelengths is below 15%. The increase in both visible and infrared absorptance exhibited by these samples is nearly identical to the increase of absorptance we reported for sulfur hexafluoride and hydrogen sulfide gas [1]. In each figure the dashed curves show the absorptance of the chalcogen-doped substrates after annealing for 30 min at 775 K in vacuum. For all three samples the absorptance of visible wavelengths is largely unaffected by annealing; however, annealing reduces the absorptance at wavelengths between 1.2 to 2.5 μm by a different amount depending on the chalcogen dopant used. The absorptance changes from an initial value of 0.9 for all three dopant

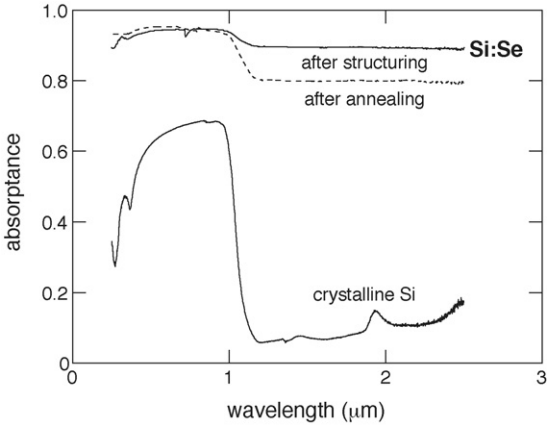

Fig. 3. Absorptance spectra for a sample doped with selenium before annealing (solid black line), and after annealing to 775 K for 30 min (dashed line). The absorptance of an untreated silicon wafer is included for comparison.

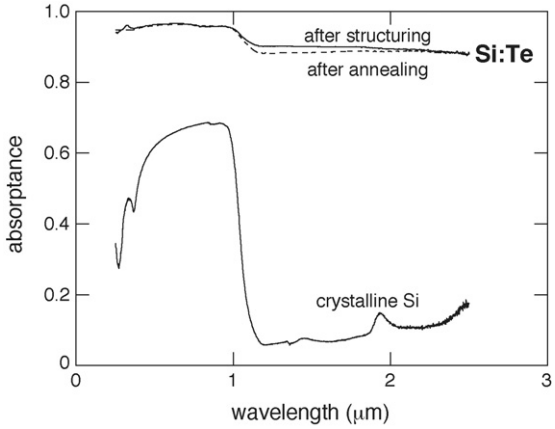

Fig. 4. Absorptance spectra for a sample doped with tellurium before annealing (solid black line), and after annealing to 775 K for 30 min (dashed line). The absorptance of an untreated silicon wafer is included for comparison.

Table 1
Rutherford backscattering analysis results

Sample	Layer	Thickness[a] (nm)	Concentration (at.%)
Sulfur	1	200	1
Sulfur, annealed	1	200	1
Selenium	1	200	0.7
Selenium, annealed	1	200	0.7
Tellurium	1	20	7
	2	200	1.5
Tellurium, annealed	1	200	1.3

[a] Layer thickness is qualitative. Transmission electron microscopy results indicate that the damaged layer is about 300 nm thick [22].

types to 0.48, 0.8 and 0.89, for sulfur, selenium and tellurium dopants, respectively.

The results of the Rutherford backscattering analysis are summarized in Table 1. The samples doped with sulfur contain about 1 at.% sulfur in a layer that is 200 nm thick, before and after annealing. The selenium doped samples both contain approximately 0.7% selenium. Prior to annealing, the tellurium spectrum is best fit by a simulated spectrum of two surface layers. The outermost layer is approximately 20 nm thick and contains 7% tellurium; the next layer is 200 nm thick and contains 1.5% tellurium. After annealing the spectrum can be simulated with only one layer that is 200 nm thick and contains 1.3% tellurium.

4. Discussion

The morphology of the microstructured samples (Fig. 1) evolves by ablation with several hundred femtosecond-laser pulses and is similar in appearance to our previous research on samples made in different background gases [1,24]. The physical mechanism governing the formation of conical structures after irradiation with several hundred femtosecond-laser pulses is addressed elsewhere [28,29].

For each of the chalcogen-doped substrates, the absorptance of visible wavelengths is increased to ~0.95 after femtosecond-laser irradiation. We have observed this same result in all our

previous work using many different gases as the dopant source (e.g. SF_6, H_2S, Cl_2, H_2, air, N_2) [1,23–25] regardless of whether the doped substrates do or do not exhibit below band gap infrared absorptance. When irradiation is performed in vacuum, the absorptance of visible light is increased to the same value of 0.95 [28]. In all cases, the enhanced visible absorptance is unaffected by annealing [1,23,25,28]. Based on these results, we attribute the enhanced visible absorptance to amplification of the intrinsic visible absorptance of ordinary silicon by multiple reflections on the textured surface. The mechanism governing below band gap infrared absorptance will be discussed below.

The RBS data in Table 1 indicates that our doping process, using a powder source, does indeed form a thin highly doped surface layer on the silicon wafer for each of the chalcogen dopants just as in the case of sulfur hexafluoride and hydrogen sulfide gas [1,23]. The estimated thickness of the layer agrees well with the laser-modified thickness of other silicon samples irradiated in gas using similar laser conditions as determined by cross-section transmission electron microscopy [23]. The RBS data of the tellurium doped sample before annealing shows an extremely high concentration of tellurium (7%) in a 20 nm thick layer, which disappears after annealing. We attribute this layer to a tellurium powder residue left after irradiation, which desorbs upon annealing.

Whether the dopant source is a background gas or a solid powder, the mechanism for trapping the dopant atoms in the silicon substrate is likely the same. During irradiation with ultrashort laser pulses above the ablation threshold, the top layer of silicon is ablated away and the next layer below melts. This thin molten layer solidifies with an extremely high resolidification velocity [30]. As a result it is possible to trap a high concentration of dopant species in the newly crystallized silicon layer resulting in a supersaturated solution. Solute trapping in this manner is known to occur after short pulsed laser annealing of silicon [31] and germanium [32] ion-implanted with impurity species. Ion implantation deposits a high concentration of dopants in the surface layer (orders of magnitude above the solubility limit) but also disorders the material leaving it mostly amorphous. Irradiation with short laser pulses recrystallizes the material, trapping the high concentration of dopants in the lattice. Solute trapping in this manner has been investigated extensively [33,34]. We propose that upon femtosecond-laser irradiation of silicon coated with the chalcogen dopant, the thin molten layer left behind contains a high concentration of chalcogens and this high concentration persists in the nanometer-sized grains after resolidification via a similar mechanism to short pulse laser irradiation of ion-implanted material. Another result of the rapid resolidification is a high density of point defects (vacancies and interstitials) [35]. The end result is a polycrystalline surface layer with a supersaturated concentration of dopants and point defects.

We believe that the supersaturated concentration of dopant atoms and point defects in the silicon lattice gives rise to the near-unity absorption of below band gap radiation exhibited in Figs. 2–4. Previous studies have shown that doping silicon with a chalcogen using thermal diffusion, which inherently restricts the concentration to the solubility limit, creates discrete states in the band gap [18,36]. The number and energy of these states vary with the chalcogen used. However, they all create deep levels in the band gap of silicon, where the deepest-lying state is 0.614, 0.593 and 0.411 eV below silicon's conduction band edge for the dopants of sulfur, selenium, and tellurium, respectively. The highest measured solubility limit of either sulfur, selenium or tellurium in silicon is approximately 10^{17} cm^{-3} for selenium [14,16,19]. In contrast, we measure chalcogen concentrations of 0.7–1.3% or about 10^{20} cm^{-3}. Results from our past work using sulfur hexafluoride gas as the dopant source, indicate that 20–70% of the sulfur atoms implanted with our process are substitutional in the lattice [22]. If 20% of the chalcogen dopant atoms are substitutionally located in the lattice, we obtain a soluble concentration of chalcogen atoms of about 10^{19} cm^{-3} which is still several orders of magnitude higher than the solid solubility limit. We propose that this supersaturated solution of chalcogen dopants in the silicon lattice creates one or more impurity bands [37] around the discrete states observed in the thermal doping of crystalline silicon [18] and these impurity bands are responsible for the absorption of below band gap radiation. In addition, a recent theoretical study shows that various combinations of sulfur atoms and point defects in the silicon lattice – such as vacancies, dangling bonds and floating bonds – result in several mid-band gap states [38]. Therefore, the absorption of below band gap radiation exhibited by our samples is likely caused by the formation of mid-band gap impurity bands created by a high concentration of dopant atoms and other lattice defects.

Our annealing data supports our proposed explanation for the absorption of below band gap radiation. After irradiation, the silicon lattice is in a highly non-equilibrium state due to the high concentration of defects. During annealing, the material moves to a more thermodynamically favorable state. The supersaturated dopants and defects diffuse out of the crystalline grains to the grain boundaries. As the defects reach the grain boundaries they no longer contribute to impurity bands in the silicon and the absorption of below band gap radiation is reduced. After annealing, the absorptance for near infrared wavelengths of samples doped with sulfur, selenium and tellurium decreases from a high value of 0.9 to a lower value of 0.48, 0.8 and 0.89, respectively. This trend correlates well with the diffusivity, D, of each dopant in a crystalline silicon lattice at 775 K as seen in Table 2 (i.e. higher diffusivity results in a greater diffusion length, and therefore has a greater impact on the optical properties). The listed values of the diffusivities at 775 K are linearly extrapolated from an Arrhenius plot ($\log D$ versus $1/T$) of data from various experimental studies showing the diffusivity of sulfur, selenium and tellurium over the temperature range 1100–1600 K (data obtained from Fig. 3 of Ref. [19]). In this temperature range, bulk diffusion is the dominant mechanism. At lower tempera-

Table 2
Diffusion data for chalcogens in silicon

Dopant element	Bulk diffusivity in c-Si at $T = 775$ K ($cm^2\ s^{-1}$)	Estimated diffusion length (nm)
S	4×10^{-15}–7×10^{-15}	27–35
Se	8×10^{-19}–3×10^{-17}	0.4–2.3
Te	1×10^{-22}	0.004

tures, bulk diffusion data are usually not valid as other diffusion mechanisms, such as grain boundary diffusion, contribute to mass flow resulting in a higher diffusivity. However, we believe that this extrapolation is valid, as it is the bulk diffusion of the dopant atoms through the bulk of the crystalline grains to the grain boundaries that reduces the infrared absorptance. Although grain boundary diffusion may occur, once the defects reach the grain boundary they no longer contribute to the infrared absorptance, and therefore grain boundary diffusion would not affect infrared absorptance. The approximate diffusion length, d, for a dopant atom after annealing can be estimated using, $d = (Dt)^{1/2}$, and resulting values for $t = 30$ min at 775 K are listed in Table 2. Given that the grain size is 10–50 nm [23], these diffusion lengths are the right order of magnitude to support that diffusion of dopant atoms and defects to the grain boundaries is the cause of the observed decrease in near infrared absorption.

The above analysis is consistent with the unchanged concentration of dopant atoms (as measured by RBS) after annealing, even though the absorption of below band gap radiation is decreased. The RBS measurement detects dopant atoms both inside the grain and at grain boundaries. While annealing does result in microscopic diffusion of dopant atoms out of grains, there is not enough time and energy for macroscopic diffusion of dopants out of the probe depth of the RBS measurement.

The tellurium and selenium samples have great potential for use in infrared photodetectors that require an annealing step during manufacture. We have previously shown that samples doped with sulfur using femtosecond-laser irradiation can be successfully used in an infrared photodetector [2]. A key manufacturing step is a thermal anneal that enhances the diodic nature of the detector; however, this anneal decreases the detector's absorption in the infrared. Samples doped with selenium or tellurium offer the potential to increase the responsivity of silicon-based photodetectors even further than samples doped with sulfur.

5. Conclusion

In conclusion, doping of silicon using sulfur, selenium, and tellurium powder leads to near-unity absorption of below band gap radiation. We attribute the near-unity absorptance to a supersaturated solution of trapped chalcogen dopants and point defects in the silicon lattice, which modifies the electronic structure of the surface layer. Annealing the samples results in diffusion of chalcogen dopants and point defects out of the crystalline grains to the grain boundaries. As a result of this annealing the absorptance of below band gap radiation is reduced by an amount that correlates to the diffusivity of the dopant atom in silicon. Samples doped with tellurium and selenium show the least reduction of infrared absorptance upon annealing and offer the potential for high responsivity silicon-based photodetectors, where annealing is often a necessary manufacturing step.

Acknowledgements

Several people contributed to the work described in this paper. Michael A. Sheehy designed and carried out the experiment, and performed the numerical fitting. Michael A. Sheehy and Brian R. Tull analyzed and interpreted the results. Eric Mazur and Cynthia M. Friend supervised the research and contributed to the development of the manuscript. Michael A. Sheehy wrote the first draft of the manuscript. Brian R. Tull extensively revised this draft to produce the current version. All authors subsequently revised and approved the final manuscript. James E. Carey, Iva Z. Maxwell and Mark T. Winkler provided feedback on the manuscript throughout its development. The research described in this paper was supported by the Department of Energy under contract DOE DE-FC36-01G011051 and the Army Research Office under contract ARO W911NF-05-1-0341.

References

[1] M.A. Sheehy, L. Winston, J.E. Carey, C.M. Friend, E. Mazur, Chem. Mater. 17 (2005) 3582–3586.
[2] J.E. Carey, C.H. Crouch, M. Shen, E. Mazur, Opt. Lett. 30 (2005) 1773–1775.
[3] Y.A. Astrov, L.M. Portsel, A.N. Lodygin, V.B. Shuman, E.V. Beregulin (Eds.), Gettering and Defect Engineering in Semiconductor Technology Xi, 2005, pp. 401–406.
[4] N. Sclar, J. Appl. Phys. 52 (1981) 5207–5217.
[5] T.G. Brown, D.G. Hall, Appl. Phys. Lett. 49 (1986) 245–247.
[6] T.G. Brown, P.L. Bradfield, D.G. Hall, Appl. Phys. Lett. 51 (1987) 1585–1587.
[7] A. Henry, J. Svensson, E. Janzen, B. Monemar, Mater. Sci. Eng. B-Solid State Mater. Adv. Technol. 4 (1989) 261–264.
[8] X. Zhang, M. Kleverman, J. Olajos, Semicond. Sci. Technol. 14 (1999) 1076–1079.
[9] M.A. Lourenco, M. Milosavljevic, S. Galata, M.S.A. Siddiqui, G. Shao, R.M. Gwilliam, K.P. Homewood, Vacuum 78 (2005) 551–556.
[10] S.K. Sharma, J. Baveja, R.M. Mehra, Phys. Status Solidi a-Appl. Res. 194 (2002) 216–225.
[11] R.M. Mehra, J. Baveja, L.P. Purohit, R. Kumar, A.V. Singh, P.C. Mathur, P.C. Taylor, J. Non-Cryst. Solids 266 (2000) 708–712.
[12] G.H. Lin, M.Z. He, J.O. Bockris, Sol. Energy Mater. Sol. Cells 44 (1996) 157–164.
[13] S.L. Wang, J.M. Viner, M. Anani, P.C. Taylor, J. Non-Cryst. Solids 166 (1993) 251–254.
[14] A.A. Taskin, B.A. Zaitsev, V.I. Obodnikov, E.G. Tishkovskii, Semiconductors 34 (2000) 312–318.
[15] F. Rollert, N.A. Stolwijk, H. Mehrer, Mater. Sci. Eng. B-Solid State Mater. Adv. Technol. 18 (1993) 107–114.
[16] R.G. Wilson, J. Appl. Phys. 55 (1984) 3490–3494.
[17] S.U. Campisano, G. Foti, P. Baeri, M.G. Grimaldi, E. Rimini, Appl. Phys. Lett. 37 (1980) 719–722.
[18] E. Janzen, R. Stedman, G. Grossmann, H.G. Grimmeiss, Phys. Rev. B 29 (1984) 1907–1918.
[19] E. Janzen, H.G. Grimmeiss, A. Lodding, C. Deline, J. Appl. Phys. 53 (1982) 7367–7371.
[20] H.R. Vydyanath, J.S. Lorenzo, F.A. Kroger, J. Appl. Phys. 49 (1978) 5928–5937.
[21] P.G. Carey, T.W. Sigmon, Appl. Surf. Sci. 43 (1989) 325–332.
[22] C.H. Crouch, J.E. Carey, J.M. Warrender, M.J. Aziz, E. Mazur, F.Y. Genin, Appl. Phys. Lett. 84 (2004) 1850–1852.
[23] C.H. Crouch, J.E. Carey, M. Shen, E. Mazur, F.Y. Genin, Appl. Phys. A 79 (2004) 1635–1641.
[24] R.J. Younkin, J.E. Carey, E. Mazur, J.A. Levinson, C.M. Friend, J. Appl. Phys. 93 (2003) 2626–2629.
[25] C. Wu, C.H. Crouch, L. Zhao, J.E. Carey, R.J. Younkin, J.A. Levinson, E. Mazur, R.M. Farrel, P. Gothoskar, A. Karger, Appl. Phys. Lett. 78 (2001) 1850–1852.
[26] T.-H. Her, R.J. Finlay, C. Wu, E. Mazur, Appl. Phys. A 70 (2000) 383–385.
[27] T.-H. Her, R.J. Finlay, C. Wu, S. Deliwala, E. Mazur, Appl. Phys. Lett. 73 (1998) 1673–1675.

[28] J.E. Carey, Harvard University, 2004.
[29] B.R. Tull, J.E. Carey, E. Mazur, J. McDonald, S.M. Yalisove, Matter. Res. Soc. Bull. 31 (2006) 626–633.
[30] P.H. Bucksbaum, J. Bokor, Phys. Rev. Lett. 53 (1984) 182–185.
[31] C.W. White, S.R. Wilson, B.R. Appleton, F.W. Young, J. Appl. Phys. 51 (1980) 738–749.
[32] E.M. Lawson, J. Appl. Phys. 53 (1982) 6459–6460.
[33] K.A. Jackson, G.H. Gilmer, H.J. Leamy, in: C.W. White, P.S. Peercy (Eds.), Laser and Electron Beam Processing of Materials, Academic Press, New York, 1980, p. 104.
[34] J.W. Cahn, S.R. Coriell, W.J. Boettinger, in: C.W. White, P.S. Peercy (Eds.), Laser and Electron Beam Processing of Materials, Academic Press, New York, 1980, p. 89.
[35] V.I. Emel'yanov, D.V. Babak, Appl. Phys. A-Mater. Sci. Process. 74 (2002) 797–805.
[36] H.G. Grimmeiss, E. Janzen, H. Ennen, O. Schirmer, J. Schneider, R. Worner, C. Holm, E. Sirtl, P. Wagner, Phys. Rev. B 24 (1981) 4571–4586.
[37] J.I. Pankove, Optical Processes in Semiconductors, Dover Publications, Inc., New York, 1971.
[38] Y. Mo, M.Z. Bazant, E. Kaxiras, Phys. Rev. B 70 (2004).